

# Temperature-tuned band gap energy and oscillator parameters of $\text{GaS}_{0.5}\text{Se}_{0.5}$ single crystals



Mehmet Isik<sup>a,\*</sup>, Evrin Tugay<sup>b</sup>, Nizami Gasanly<sup>c,d</sup>

<sup>a</sup> Department of Electrical and Electronics Engineering, Atilim University, 06836 Ankara, Turkey

<sup>b</sup> Department of Mechanical Engineering, Recep Tayyip Erdogan University, 53100 Rize, Turkey

<sup>c</sup> Department of Physics, Middle East Technical University, 06800 Ankara, Turkey

<sup>d</sup> Virtual International Scientific Research Centre, Baku State University, 1148 Baku, Azerbaijan

## ARTICLE INFO

### Article history:

Received 19 April 2016

Accepted 8 June 2016

### Keywords:

Semiconductors

Optical properties

Absorption

## ABSTRACT

Temperature-dependent transmission and room temperature reflection measurements were carried out on  $\text{GaS}_{0.5}\text{Se}_{0.5}$  single crystal in the wavelength range of 380–1000 nm to investigate its optical parameters. The analysis of the temperature-dependent absorption data showed that direct and indirect band gap energies increase from 2.36 to 2.50 eV and 2.27 to 2.40 eV, respectively, as temperature is decreased from 300 to 10 K. The rates of change of the direct and indirect band gap energies with temperature was found around  $-7.4 \times 10^{-4}$  eV/K from the analysis of experimental data under the light of theoretical relation giving the band gap energy as a function of temperature. The absolute zero value of the band gap energies were also found from the same analysis as 2.50 eV (for direct) and 2.40 eV (for indirect). Wemple-DiDomenico single effective oscillator model, Sellmeier oscillator model and Spitzer-Fan model were used for the room temperature reflection data to find optical parameters of the crystal.

© 2016 Elsevier GmbH. All rights reserved.

## 1. Introduction

The semiconducting crystals designated with chemical formula of  $\text{GaX}$  (where  $X = \text{S}, \text{Se}$  or  $\text{Te}$ ) have become interesting due to their attractive properties in optoelectronic applications. The members of this group,  $\text{GaSe}$  and  $\text{GaS}$ , take attention of researchers because of their potential usage in optoelectronic devices operating in red and blue visible regions [1–3]. The studies on technological applications of these crystals showed that  $\text{GaSe}$  can be a promising material used in nonlinear optical applications [4], far-infrared conversion applications [5] and heterostructure devices [6] whereas  $\text{GaS}$  takes interest for near-blue light emitting devices [7]. A recent paper on these crystals reported the results of studies on possible usage of  $\text{GaSe}/\text{GaS}$  as ultrathin layer transistors [8].

$\text{GaSe}$  and  $\text{GaS}$  crystals have hexagonal structures with lattice parameters of  $a = 0.375$  nm,  $c = 1.595$  nm (for  $\text{GaSe}$ ) and  $a = 0.359$  nm,  $c = 1.549$  nm (for  $\text{GaS}$ ) [9,10]. The optical characterization of  $\text{GaSe}$  single crystal showed that it has 2.117 and 2.169 eV direct and indirect band gap energies, respectively, at 77 K [11] and 1.988 eV band gap energy at room temperature [12].  $\text{GaS}$  is a wide band gap semiconductor having indirect and direct gap energies of 2.59 eV and 3.04 eV, respectively, at room temperature [13].  $\text{GaSe}$  and  $\text{GaS}$  crystals form  $\text{GaS}_x\text{Se}_{1-x}$  ( $0 \leq x \leq 1$ ) mixed crystals which were investigated in recent studies from the point view of structural [14] and optical [15] properties in the regions of ( $0 \leq x \leq 0.5$ ). In the mentioned

\* Corresponding author.

E-mail address: [mehmet.isik@atilim.edu.tr](mailto:mehmet.isik@atilim.edu.tr) (M. Isik).

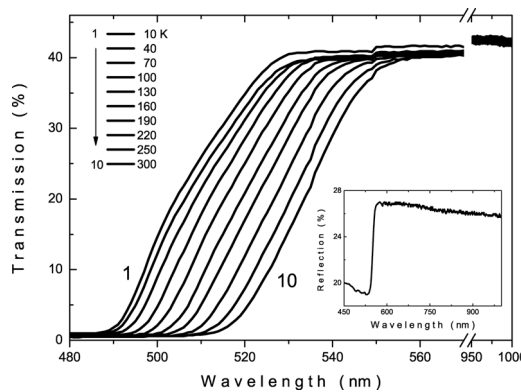


**Fig. 1.** The spectral dependence of transmission for  $\text{GaS}_{0.5}\text{Se}_{0.5}$  crystal in the temperature range of 10–300 K. Inset: the spectral dependence of reflectivity at room temperature.

studies, the variation of lattice parameters and band gap energy with composition were reported. Previously, our research group reported the results of ellipsometry measurements carried out on  $\text{GaS}_x\text{Se}_{1-x}$  mixed crystals in the composition range of  $0 \leq x \leq 1$  [16]. The variation of interband transition energies with composition was revealed. The results of transmission, piezoreflectance and ellipsometry measurements on the mixed crystals showed that band gap and interband transition energies show nearly an increasing behavior as sulfur composition is increased in the mixed crystals.

In the compositional range ( $0 \leq x \leq 1$ ) of mixed crystals,  $\text{GaS}_{0.5}\text{Se}_{0.5}$  is the most distinctive crystal showing properties of  $\text{GaSe}$  and  $\text{GaS}$ . Under the light of technological potentials of constituent compounds  $\text{GaSe}$  and  $\text{GaS}$ , mixed crystal  $\text{GaS}_{0.5}\text{Se}_{0.5}$  can be thought as an attractive candidate in the areas of light emitting devices, optical detecting systems and fabrication of long-pass filters. The layered structured crystal has four atomic planes with the sequence  $\text{Se}(\text{S}) - \text{Ga} - \text{Ga} - \text{Se}(\text{S})$ . Previously, room temperature transmission and ellipsometry experiments were accomplished on the  $\text{GaS}_{0.5}\text{Se}_{0.5}$  crystal to investigate its optical properties. The direct and indirect band gap energies of the crystals were found as 2.28 eV and 2.38 eV, respectively, from the analysis of room temperature transmission and reflection measurements [17]. The results of ellipsometry experiments performed in the 1.2–6.0 eV spectral region to reveal the interband transition energies showed that there exist five transition with energies ranging from 3.87 to 5.34 eV [17]. The aim of the present work is to expand the optical characterization studies on  $\text{GaS}_{0.5}\text{Se}_{0.5}$  crystal by performing temperature-dependent transmission measurements in the 10–300 K range. Absolute zero value of the band gap energy, the rate of change in the band gap energy and Debye temperature were obtained from the analysis of dependence of band gap energies on temperature. Moreover, Wemple-DiDomenico single effective oscillator model, Sellmeier oscillator model and Spitzer-Fan model were applied to the room temperature reflection experimental data to find optical parameters of the crystal.

## 2. Experimental details

$\text{GaS}_{0.5}\text{Se}_{0.5}$  polycrystals were synthesized from high-purity elements (at least 99.999%) prepared in stoichiometric proportions. Single crystals of  $\text{GaS}_{0.5}\text{Se}_{0.5}$  were grown by the Bridgman method in evacuated ( $10^{-5}$  Torr) silica tubes (10 mm in diameter and about 25 cm in length) with a tip at the bottom in our crystal growth laboratory. The ampoule was moved in a vertical furnace through a thermal gradient of 30 °C/cm, between the temperatures 1000 and 650 °C at a rate of 0.5 mm/h. The samples were prepared by easy cleavage an ingot parallel to the crystal layer (perpendicular to the *c*-axis). The chemical composition of the crystals,  $\text{Ga:S:Se}$ , was found from the energy dispersive spectroscopy measurements as 49.8:24.8:25.4 [17]. Transmission and reflection measurements were carried out in the 380–1000 nm spectral range using Shimadzu UV 1201 model spectrophotometer with resolution of 5 nm, which consisted of a 20 W halogen lamp, a holographic grating and a silicon photodiode. Transmission measurements were performed under normal incidence of light with a polarization direction along the (001) plane. This plane is perpendicular to the *c*-axis of the crystal. For the reflection experiments, a specular reflectance measurement attachment with a 5° incident angle was used. Temperature-dependent transmission measurements were performed in the 10–300 K range using Advanced Research Systems, Model CSW-202 closed cycle helium cryostat to cool the sample. Accuracy of the cooling system was 0.5 K. Reflection experiments were only done at room temperature since technical reasons related to usage of cryostat did not allow us to perform the measurements at low temperatures.

## 3. Results and discussion

Fig. 1 shows the temperature dependence of transmittance ( $T$ ) spectra of  $\text{GaS}_{0.5}\text{Se}_{0.5}$  single crystals in the wavelength ( $\lambda$ ) range of 480–1000 nm and temperature range of 10–300 K. Room temperature reflectance ( $R$ ) spectra were obtained using

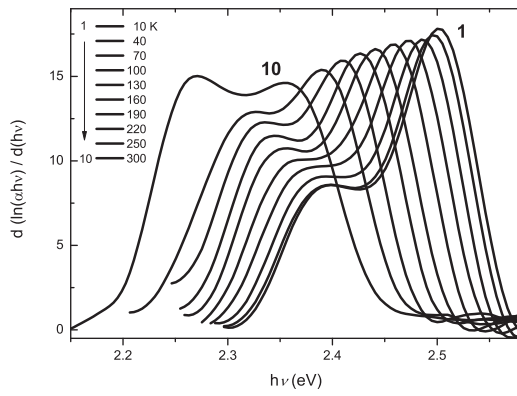


**Fig. 2.** The dependence of  $d(\ln(\alpha h\nu))/d(h\nu)$  on photon energy for  $\text{GaS}_{0.5}\text{Se}_{0.5}$  crystal in the temperature range of 10–300 K.

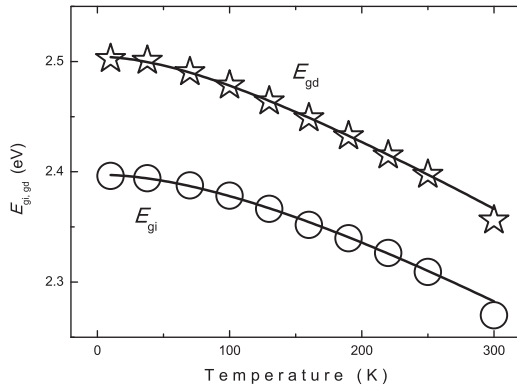


**Fig. 3.** The direct (stars) and indirect (circles) band gap energies as a function of temperature. The solid lines are fitted lines.

samples with natural cleavage planes and thickness ( $d$ ) such that  $\alpha d \gg 1$  (inset of Fig. 1) where  $\alpha$  symbolize absorption coefficient calculated using the expression [18]

$$\alpha = \frac{1}{d} \ln \left\{ \frac{(1-R)^2}{2T} + \left[ \frac{(1-R)^4}{4T^2} + R^2 \right]^{1/2} \right\}. \quad (1)$$

Thickness of the used sample for temperature-dependent transmission experiments was measured as  $80 \mu\text{m}$ . It was not possible to perform temperature-dependent reflection experiments in our cryostat system. Therefore, a room temperature reflectivity spectrum was uniformly shifted in energy according to the blue shift of the absorption edge for calculation of absorption coefficient at low temperatures. Dependence of  $\alpha$  on photon energy ( $h\nu$ ) is given as [18]

$$(\alpha h\nu) = A(h\nu - E_g)^p \quad (2)$$

where  $A$  is a constant depending on transition probability,  $E_g$  is the band gap energy and  $p$  is an index which is equal to 2 and 1/2 for indirect and direct transitions, respectively. Absorption coefficient and photon energy given by Eq. (2) can also be related with each other as [19]

$$\frac{d \ln(\alpha h\nu)}{d(h\nu)} = \frac{p}{h\nu - E_g}. \quad (3)$$

This equation points out that  $d(\ln(\alpha h\nu))/d(h\nu)$  vs.  $(h\nu)$  plot exhibits a peak at energy having its maximum intensity at band gap energy value. Fig. 2 presents the related plots at used temperatures for experiments. As can be seen from the figure, there exist two peaks at each temperature. The behavior of the transition for observed peaks was revealed from the slope ( $p$ ) of  $\ln(\alpha h\nu)$  versus  $\ln(h\nu - E_g)$  graphs which indicated the presence of indirect transitions for peaks at lower energy ( $p \approx 2$ ) and direct transitions for peaks at higher energy ( $p \approx 0.5$ ). Results of analyses showed that direct ( $E_{gd}$ ) and indirect ( $E_{gi}$ ) band gap energies increases from 2.36 to 2.50 eV and 2.27 eV to 2.40 eV, respectively, as temperature is decreased from 300 to 10 K (see Fig. 3). Temperature dependence of the band gap energies was analyzed using the expression [18]

$$E_g(T) = E_g(0) + \frac{\gamma T^2}{T + \beta}. \quad (4)$$

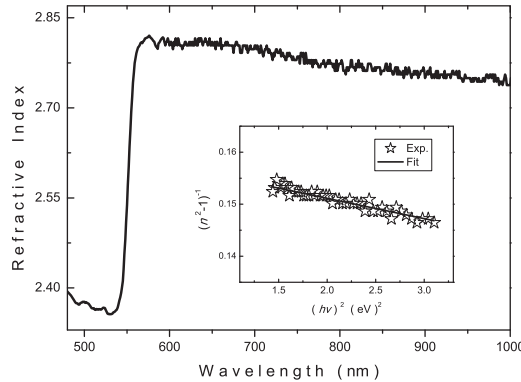


**Fig. 4.** The variation of refractive index as a function of wavelength at room temperature. Inset: the plot of  $(n^2 - 1)^{-1}$  vs.  $(hv)^2$  in the  $h\nu < E_g$  range. Stars are experimental data and solid line represents the linear fit.

where  $E_g(0)$  is absolute zero value of band gap,  $\gamma$  is rate of change of the band gap with temperature and  $\beta$  is Debye temperature. Fig. 3 shows the fit (solid lines) of experimental data (open circles and stars) accomplished using Eq. (4). The fitting process resulted with  $E_{gi}(0)=2.40\text{ eV}$  and  $E_{gd}(0)=2.50\text{ eV}$  and  $\gamma$  is found around  $-7.4 \times 10^{-4}\text{ eV/K}$  for both transitions.

Fig. 4 shows the spectral dependence of room temperature refractive index obtained using the expression [18]

$$n = \frac{1+R}{1-R} + \left[ \frac{4R}{(1-R^2)} - \left( \frac{\alpha\lambda}{4\pi} \right)^2 \right]^{1/2}. \quad (5)$$

It will be worthwhile to compare refractive index of  $\text{GaS}_{0.5}\text{Se}_{0.5}$  single crystals with those of  $\text{GaSe}$  and  $\text{GaS}$ . According to Ref. [20], the refractive indices of  $\text{GaSe}$  and  $\text{GaS}$  in the 800–1000 nm spectral region which is the common range of present and referenced works vary in the 2.81–2.86 and 2.63–2.66 range, respectively. Refractive index values of  $\text{GaS}_x\text{Se}_{1-x}$  mixed crystals were given in the same work as

$$n^2(\text{GaS}_x\text{Se}_{1-x}) = xn^2(\text{GaS}) + (1-x)n^2(\text{GaSe}) \quad (6)$$

Refractive index of  $\text{GaS}_{0.5}\text{Se}_{0.5}$  single crystals changes between 2.72 and 2.76 according to Eq. (6). The spectra shown in Fig. 4 give refractive index between 2.74 and 2.77 values which are in good agreement with reported values. The spectral dependence of refractive index in the below band gap energy region was analyzed using single effective oscillator model suggested by Wemple and DiDomenico and Sellmeier oscillator model. Refractive index is related to photon energy  $h\nu$  in the single oscillator model by [21]

$$n^2(h\nu) = 1 + \frac{E_{so}E_d}{E_{so}^2 - (h\nu)^2} \quad (7)$$

where  $E_{so}$  and  $E_d$  represent the single oscillator energy and dispersion energy, respectively, which can be obtained from  $(n^2 - 1)^{-1}$  vs.  $(h\nu)^2$  plot as shown in the inset of Fig. 4. Using the slope of linear fit (solid line) and intersection point of fitted line with vertical axis, the oscillator parameters were found as  $E_{so}=6.4\text{ eV}$  and  $E_d=40.1\text{ eV}$ . Using these oscillator parameters and  $h\nu=0$  value in Eq. (7), zero-frequency refractive index ( $n_0$ ) and dielectric constant ( $\varepsilon_0$ ) were found as  $n_0=2.7$  and  $\varepsilon_0=n_0^2=7.29$ . In the Sellmeier oscillator model, refractive index is related to oscillator strength ( $S_{so}$ ) and wavelength ( $\lambda_{so}$ ) by expression [22]

$$(n^2 - 1)^{-1} = \frac{1}{S_{so}\lambda_{so}^2} - \frac{1}{S_{so}\lambda^2}. \quad (8)$$

$S_{so}$  and  $\lambda_{so}$  values of  $\text{GaS}_{0.5}\text{Se}_{0.5}$  single crystals were found from the  $(n^2 - 1)^{-1}$  vs.  $\lambda^{-2}$  curve as  $1.67 \times 10^{14}\text{ m}^{-2}$  and  $1.94 \times 10^{-7}\text{ m}$ , respectively.

The wavelength dependence of real component ( $\varepsilon_1$ ) of dielectric function was plotted using refractive index and extinction coefficient (see Fig. 5) and analyzed using Spitzer-Fan model in which  $\varepsilon_1$  is defined as [18]

$$\varepsilon_1 = n^2 - k^2 = \varepsilon_\infty - \left[ \frac{e^2}{\pi c^2} \right] \left( \frac{N}{m^*} \right) \lambda^2 \quad (9)$$

where  $\varepsilon_\infty$  is the high-frequency dielectric constant in the absence of any contribution from free carriers,  $N$  is the carrier concentration,  $m^*$  is the effective mass,  $c$  is the speed of light and  $e$  is the electronic charge. Inset of Fig. 5 presents the linear fit (solid line) of experimental data (stars).  $\varepsilon_\infty$  and  $N/m^*$  were obtained from the intersection of fitted line with  $\varepsilon_1$ -axis and slope of the linear fit, respectively, as  $\varepsilon_\infty=7.9$  and  $N/m^*=4.7 \times 10^{47}\text{ g}^{-1}\text{ cm}^{-3}$ .

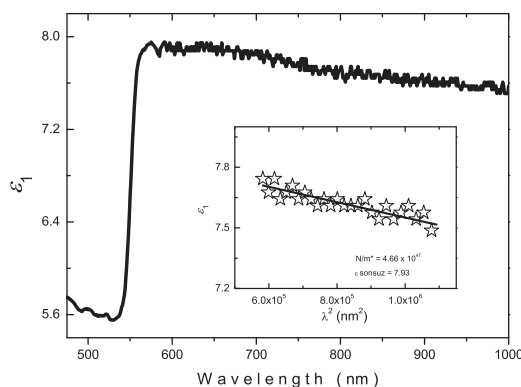


**Fig. 5.** The wavelength dependence of real component of dielectric function at room temperature. Inset: plot of  $\epsilon_1$  vs.  $\lambda^2$  in the  $h\nu < E_g$  range. Stars are experimental data and solid line shows the linear fit.

#### 4. Conclusion

Optical parameters of  $\text{GaS}_{0.5}\text{Se}_{0.5}$  single crystals were found from the analyses of temperature-dependent transmission and room temperature reflection experiments using different theoretical models. The analyses of temperature dependent absorption coefficient in the 10–300 K region revealed the presence of both of direct and indirect transitions. Direct and indirect band gap energies were found as increasing from 2.36 to 2.50 eV and 2.27 eV to 2.40 eV, respectively, as temperature is decreased from 300 to 10 K. Fitting process of the temperature dependence of band gap energy under the light of theoretical model resulted with absolute zero value of the indirect and direct band gap energies as 2.40 and 2.50 eV, respectively. Spectral dependence of refractive index was investigated in the energy region of  $h\nu < E_g$  using single effective oscillator model and Sellmeier oscillator model. Moreover, the real component of the dielectric function was analyzed using Spitzer-Fan model. The single oscillator energy, dispersion energy, oscillator strength, oscillator wavelength, high-frequency dielectric constant and ratio of carrier concentration to the effective mass were reported in this study.

#### References

- [1] G. Micocci, A. Serra, A. Tepore, Electrical properties of n-GaSe single crystals doped with chloride, *J. Appl. Phys.* 82 (1997) 2365–2369.
- [2] A. Cingolani, A. Minafra, P. Tantalo, C. Paorici, Edge emission in GaSe and GaS, *Phys. Status Solidi A* 4 (1971) K83–K85.
- [3] M. Somogyi, Anomalous photovoltage in insulating GaSe crystals, *Phys. Status Solidi A* 7 (1971) 263–267.
- [4] N.B. Singh, D.R. Suhre, V. Balakrishna, M. Marable, R. Meyer, N. Fernelius, F.K. Hopkins, D. Zelman, Far-infrared conversion materials: gallium selenide for far-infrared conversion applications, *Prog. Cryst. Growth Ch.* 37 (1998) 47–102.
- [5] M.I. Karaman, V.P. Mushinskii, Electroluminescence of layered  $\text{Ga}_x\text{Te}_{1-x}$  crystals, *Sov. Phys. Semicond.* 4 (1970) 662–664.
- [6] M. Digiulio, G. Micocci, P. Siciliano, A. Tepore, Photoelectronic and optical properties of amorphous gallium selenide thin films, *J. Appl. Phys.* 62 (1987) 4231–4235.
- [7] N. Okamoto, N. Hara, H. Tanaka, Surface passivation of InGaP/InGaAs/GaAs pseudomorphic HEMTs with ultrathin GaS film, *IEEE Trans. Electron Dev.* 47 (2000) 2284–2289.
- [8] D.J. Late, B. Liu, J. Luo, A. Yan, H.S.S.R. Matte, M. Grayson, C.N.R. Rao, V.P. Dravid, GaS and GaSe ultrathin layer transistors, *Adv. Mater.* 24 (2012) 3549–3554.
- [9] A. Kuhn, A. Chevy, R. Chevalier, Crystal structure and interatomic distances in GaSe, *Phys. Status Solidi A* 31 (1975) 469–475.
- [10] O.Z. Alekperov, M.Z. Zarabakiev, Effect of sulfur vacancies on photoconductivity in gallium sulfide, *Inorg. Mater.* 10 (1998) 971–975.
- [11] A. Mercier, E. Mooser, J.P. Voitchovsky, Near edge optical absorption and luminescence of GaSe, GaS and of mixed crystals, *J. Lumin.* 7 (1973) 241–266.
- [12] M.K. Anis, The growth of single crystals of GaSe, *J. Cryst. Growth* 55 (1981) 465–469.
- [13] E. Auclich, J.L. Brebner, E. Mooser, Indirect energy gap in GaSe and GaS, *Phys. Status Solidi B* 31 (1969) 129–134.
- [14] C.H. Ho, C.C. Wu, Z.H. Cheng, Crystal structure and electronic structure of  $\text{GaSe}_{1-x}\text{S}_x$  series layered solids, *J. Cryst. Growth* 279 (2005) 321–328.
- [15] C.C. Wu, C.H. Ho, W.T. Shen, Z.H. Cheng, Y.S. Huang, K.K. Tiong, Optical properties of  $\text{GaSe}_{1-x}\text{S}_x$  series layered semiconductors grown by vertical Bridgman method, *Mater. Chem. Phys.* 88 (2004) 313–317.
- [16] M. Isik, N.M. Gasanly, Ellipsometric study of optical properties of  $\text{GaS}_x\text{Se}_{1-x}$  layered mixed crystals, *Opt. Mater.* 54 (2016) 155–159.
- [17] M. Isik, N.M. Gasanly, Optical characterization of  $\text{Ga}_2\text{Se}_3$  layered crystals by transmission, reflection and ellipsometry, *Mod. Phys. Lett. B* 29 (2015) 1550088(1)–1550088(10).
- [18] J.I. Pankove, *Optical Processes in Semiconductors*, Prentice Hall, New Jersey, 1971.
- [19] F. Yakuphanoglu, Electrical conductivity, optical and metal-semiconductor contact properties of organic semiconductor based on MEH-PPV/fullerene blend, *J. Phys. Chem. Solids* 69 (2008) 949–954.
- [20] K. Kato, N. Umemura, Sellmeier equations for GaS and GaSe and their applications to the nonlinear optics in  $\text{GaS}_x\text{Se}_{1-x}$ , *Opt. Lett.* 36 (2011) 746–747.
- [21] S.H. Wemple, M. DiDomenico, Behavior of electronic dielectric constant in covalent and ionic materials, *Phys. Rev. B* 3 (1971) 1338–1351.
- [22] A.K. Walton, T.S. Moss, Determination of refractive index and correction to effective electron mass in PbTe and PbSe, *Proc. Phys. Soc.* 81 (1963) 509–513.